Available online at www.sciencedirect.com

SciVerse ScienceDirect

Ceramics International 38 (2012) 1287–1293

CERAMICS INTERNATIONAL

www.elsevier.com/locate/ceramint

OH and COOH functionalized single walled carbon nanotubes-reinforced alumina ceramic nanocomposites

Ali Can Zaman [a], Cem B. Üstündağ [a,b], Figen Kaya [a], Cengiz Kaya [a,*]

[a] Department of Metallurgical and Materials Engineering, Yildiz Technical University, Davutpasa Campus, Esenler, Istanbul, Turkey
[b] Vocational School, Department of Ceramics, Yildiz Technical University, Maslak Campus, Maslak, Istanbu, Turkey

Received 28 April 2011; received in revised form 25 August 2011; accepted 1 September 2011
Available online 8 September 2011

Abstract

Alumina ceramics reinforced with 1 wt.% single-walled carbon nanotube (SWCNT) were fabricated via spark plasma sintering (SPS) of composite powders containing carboxyl (COOH) or hydroxyl (OH) group functionalized single-walled carbon nanotubes. The samples were SPS'ed at 1600 °C under 50 MPa pressure for holding time of 5 min and at a heating rate of 4 °C/s. The effects of CNT addition having different surface functional groups on microstructure, conductivity, density and hardness were reported. It was shown that nanotube addition decreased the grain sizeof alumina from 3.17 μm to 2.11 μm for COOH-SWCNT reinforcement and to 2.28 μm for COOH-SWCNT reinforcement. The hardness values of the composites are similar for all samples but there is 4.5 and 7.5 times increase in electrical conductivity with respect to monolithic alumina for COOH-SWCNT and OH-SWCNT, respectively. It was also shown by TEM and FEG SEM observations that transgranular fracture behaviour of alumina was changed to mostly intergranular fracture mode by the addition of both types of CNTs which may be due to location of CNTs along the grain boundaries. A significant grain size reduction in alumina is considered toresult fromthe suppressing effect of CNTs during sintering.

Keywords: D. Al_2O_3; Carbon nanotube; Spark plasma sintering; Functional groups

1. Introduction

Alumina has been used widely in many fields for its high corrosion and wear resistance, hardness and stability at high temperature [1,2]. In response to an applied external stress, as in the case of all ceramics, alumina exhibit little or no plastic deformation, therefore energy dissipation is limited which makes alumina quite brittle.

Carbon nanotubes (CNTs) were first discovered by Oberlin et al. [3] and aroused great interest since the rediscovery by Iijima in 1991 [4]. CNTs have great potential for tougher, stronger ceramic composites exhibiting multifunctional properties due to the high stiffness [5], high tensile strength [6], high electrical and thermal conductivities of CNTs [7,8].

Large aspect ratio (relevant to enhanced load transfer), homogeneous dispersion (agglomerates act as stress concentrating sites) and interfacial bonding must be provided for an effective reinforcement [9].

The arising problem for the CNT ceramic composites is the non-polar covalently bonded structure of CNTs exhibiting agglomeration in polar and organic solvents. Covalent functionalization is one of the ways to solubilize CNTs in which functional groups attach on to the sidewalls of CNTs' defected sites and head groups [10]. Different functional groups lead to different surface characters and hence solubility. For instance fluorinated CNTs show moderate solubility in alcoholic solvents (1 mg/ml) [11] and carboxylated CNTs exhibit high solubility in polar solvents, such as water at high pH values [12].

Spark plasma sintering (SPS) is a consolidation technique and have been widely used for CNTs composites [13,14]. SPS uses pulsed direct currents applied on a conductive die. Powders are positioned in the die and pressed uniaxially. Heating of green bodies is provided by means of joule heating [15] and therefore it is a rapid sintering process [16]. SPS was examined to obtain low grain size and high density components

* Corresponding author.
E-mail address: cngzky@yahoo.co.uk (C. Kaya).

0272-8842/$36.00
doi:10.1016/j.ceramint.2011.09.002

using suitable temperature, pressure, pulsed current, holding time, heating rate and pulse sequence combinations [15].

The homogeneous dispersion of carbon nanotubes in alumina is the critical step in obtaining composites with enhanced properties. The activation of carbon nanotubes can be achieved by the decoration of their surfaces by functional groups.

The aim of the present work is to investigate the effect of different functional groups (COOH or OH) on the dispersibility of SWCNTs in alumina matrix. It also examines the effect of surface modification of SWCNTs on the properties (grain size, hardness, conductivity, fracture mode and density) of alumina ceramics densified by SPS.

2. Material and methods

A commercial α-alumina powder having 0.2 μm average particle size was selected for the experiments (Alcoa SG 16). The data related to the purchased carbon nanotubes (Timesnano, Chengdu Organic Chemicals Co. Ltd.,) with different surface functional groups are shown in Table 1.

1 wt.% SWCNTs with two different surface functional groups were dispersed in ethanol, ball milled for 3 h and subsequently ultrasonicated for 30 min. The same procedure was applied on the monolithic alumina/ethanol suspensions. The solids-loading of α-alumina powders was 5 wt.% of the total suspensions. The SWCNTs suspension was added to α-alumina suspensions during magnetic stirring and subsequently, the obtained suspensions were ball milled for 1 h, ultrasonicated for 30 min and finally dried at 100 °C in an oven prior the sieving procedure.

The samples were SPS'ed at 1600 °C under 50 MPa pressure for holding time of 5 min using a heating rate of 4 °C/s. The sintered pellets were 20 mm in diameter and approximately 5 mm in thickness. The microstructural analysis was performed after the removal of the graphitic sheets on the surfaces of the specimens. Hardness, electrical conductivity and density measurements were performed along with FEG SEM and TEM observations.

The relative densities of the composites were calculated using the theoretical densities of alumina (3.97 g/cm^3) and SWCNTs (1.71 g/cm^3 [17]). The theoretical density of the 1 wt.% SWCNT/alumina corresponds to ∼3.9474 g/cm^3. The grain sizes of the ceramic bodies, which were polished and thermally etched at 1400 °C for 40 min were measured from the sizes of approximately 200 grains on SEM images. The densities of the compacts were determined by the Archimedes method with distilled water as the immersion medium. Electrical conductivities of the samples were measured using 2-point probe technique. The hardness tests were performed using a Vickers microhardness tester in which 10 kg load was applied for 10 s for each sample.

Table 1
The properties of the commercial single-walled carbon nanotubes with different functional groups.

Properties	Carboxyl single-wall carbon nanotubes (COOH-SWCNTs)	Hydroxyl single-wall carbon nanotubes (OH-SWCNTs)
Diameter (nm)	1–2	1–2
Length (nm)	∼30	∼30
–COOH content/–OH content (wt.%)	2.73	3.96
Purity (wt.%)	>90	>90
Ash (wt.%)	<1.5	<1.5
Electrical conductivity (S/cm)	$>10^2$	$>10^2$

3. Results and discussions

Fig. 1 shows the SEM images of fractured surfaces of monolithic Al_2O_3 and SWCNT-reinforced alumina composites. The fracture mode of monolithic Al_2O_3 is seen to be a combination of intergranular (IG) and transgranular (TG) as the coarser alumina grains fail transgranularly while the smaller grains fracture intergranularly, as shown in Fig. 1a. In Fig. 1b and c, the fracture surfaces of COOH functionalized SWCNT/Al_2O_3 are shown and Fig. 1d represents OH functionalized SWCNT/Al_2O_3. It is clearly shown in Fig. 1b and d that there is a shift in the fracture behaviour towards intergranular compared to monolithic Al_2O_3 as the surface functionalized SWCNTs are mostly located along the alumina grain boundaries (the location of the CNTs is shown by arrows in Fig. 1b and d).

It should also be noted from Fig. 1 that although the fracture mode is heavily intergranular for both CNT-reinforced alumina there are still some coarse grains that fail transgranularly, as shown in Fig. 1d. It is noted from the fracture surfaces that the grains bigger than 2 μm fracture transgranularly either in monolithic or reinforced alumina, as shown in Fig. 1.

Fig. 2 illustrates the polished surfaces of the sintered ceramic samples. As seen from the images shown in Fig. 2a and b, the average grain size of monolithic Al_2O_3 is determined to be 3.17 μm. The backscattered electron image of monolithic alumina at low magnification reveals the pattern of the polished surface by the help of the contrast between pores and the grains and this can be used as a control while comparing the composites with monolithic Al_2O_3 at low magnification in terms of the agglomerates. Fig. 2c and d shows the COOH-SWCNT/Al_2O_3 having an average grain size of 2.11 μm while Fig. 2e and f illustrates the OH-SWCNT/Al_2O_3in which the average grain size of alumina is 2.28 μm. Fig. 2g and h is the high magnification images of COOH-SWCNT/Al_2O_3 and OH-SWCNT/Al_2O_3, respectively in which it is clearly seen that carbon nanotubes emerge from grain boundaries proving their location to be along the alumina grain boundaries. The polished surfaces of both composites containing OH and COOH functionalized SWCNTs are similar in terms of grain size and morphology, as shown in Fig. 2c–h. Besides, the low magnification backscattered electron images of composites in Fig. 2d and f present the pores of agglomerates of CNTs in which CNTs are pulled out during polishing. The diameters of agglomerates having nearly spherical morphology are in the range of 10–20 μm in both composites, as shown in Fig. 2g and h. Nanotubes migrate towards the grain boundaries during the

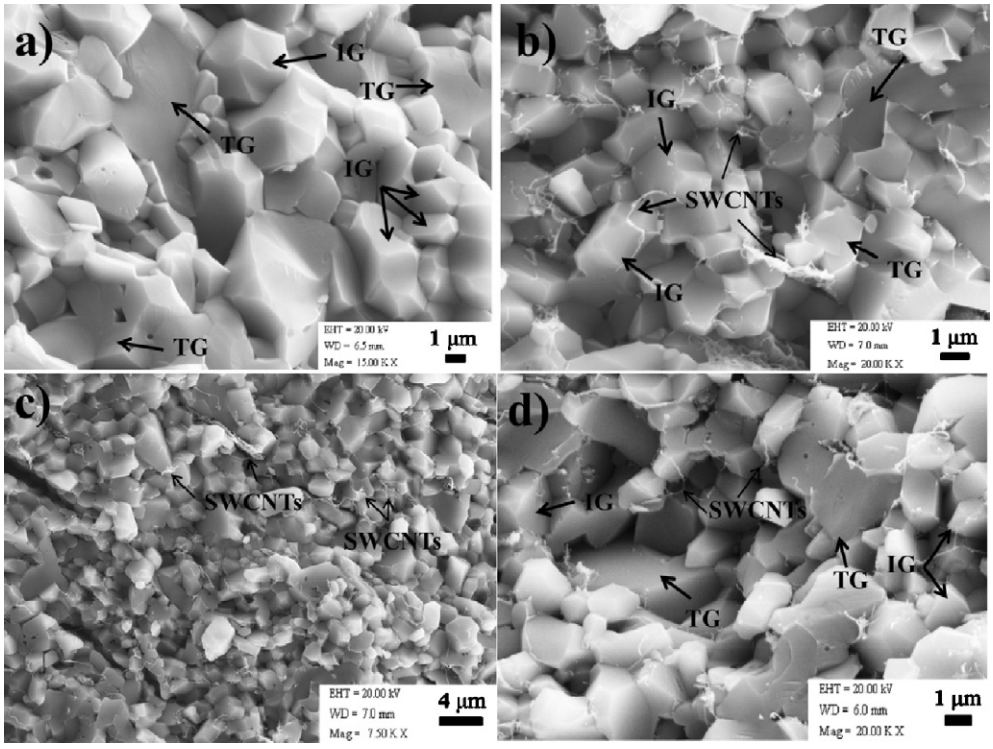

Fig. 1. The fracture surfaces of monolithic Al_2O_3 (a), COOH-SWCNT reinforced Al_2O_3 (b and c), and OH-SWCNT reinforced Al_2O_3(d). IG, intergranular fracture; TG, transgranular fracture.

grain growth of alumina resulting in a tendency to agglomerate after sintering at relatively high grain sizes [18,19].

The detail TEM microstructures of monolithic and CNTs-reinforced aluminas are shown in Fig. 3. Fig. 3a shows the clean grain boundaries of monolithic alumina. The microstructures of the COOH-SWCNT/Al_2O_3 are shown in Fig. 3b and c indicating the location of the CNTs along the grain boundaries and also at the triple grain junctions. This finding is in good agreement with the published studies [20,21] which show that carbon nanotubes tend to locate between grains which are indicated by a black arrow in the image shown in Fig. 3b. The location of the carbon nanotubes along the grains may result in higher electrical conductivity even at low CNT contents by virtue of their high aspect ratio and it may also contribute to the retardation of the grain growth [20,21]. In Fig. 3c, a more magnified case of COOH-SWCNT/Al_2O_3 is shown in which CNTs are clustered at the triple junctions. In Fig. 3d the finer grain size structure of alumina is seen for COOH-SWCNT/Al_2O_3 with the absence of any remaining porosity. Similar microstructure to COOH-SWCNT/Al_2O_3 is observed in OH-SWCNT/Al_2O_3 revealing that SWCNTs locate between grains, marked by arrows in Fig. 3e. Fig. 3e also shows the location of the CNTs to be at the triple grain junctions of alumina.

Besides, Ueda et al. used carbon nanofibres (CNFs) to fabricate CNFs-alumina composites, and they found out that there is a critical content at which carbon CNFs tend to cluster more easily between 0.8 and 1.6 wt.%. Therefore in our study to avoid excessive agglomeration SWCNTs content kept at 1 wt.% [18].

Table 2 represents collection of published data in this field and also present data obtained from the studied samples as well. The sintered monolithic Al_2O_3, 1 wt.% COOH-SWCNT/Al_2O_3 and 1 wt.% OH-SWCNT/Al_2O_3 have densities of 3.93 g/cm^3, 3.86 g/cm^3 and 3.86 cm^3, respectively. The corresponding relative densities and other properties are shown in detail in Table 2. As shown in Table 2, the relative densities (%) of monolithic alumina, 1 wt.% COOH-SWCNT/Al_2O_3 and 1 wt.% OH-SWCNT/$Al_2O_3$are determined to be 99.55, 97.78 and 97.78, respectively indicating a slight decrease by the addition of CNTs. The decrease in density is attributed to the presence of entangled CNTs that form porous agglomerates in the alumina (Fig. 1a and h). The hardness values are very close to each other for monolithic and CNTs-reinforced alumina (around 18.3 GPa for all samples) which indicate the homogeneous distribution of the CNTs within the alumina matrix (Table 2).

The sinterability of the finer grained alumina is better therefore the samples obtained by the Yamamoto et al. [22] and Zhan et al. [23] show big differences in terms of grain size and electrical conductivity and besides, it seems that the low temperatures of sintering and fine grained starting materials compared to used one in our experiments lead to decrease in grain size. The grain size refinement may influence the distribution of carbon nanotubes. Since nanotubes tend to locate along the grain boundaries, the presence of the larger surface area of the grains may influence positively in terms of the state of the dispersion of nanotubes, as they may make room for the accommodation of nanotubes causing limitation to excessive agglomeration.

Comparing the samples within each other it is seen that, there is a significant increase in electrical conductivity of alumina by the addition of SWCNTs, as shown in Table 2. The

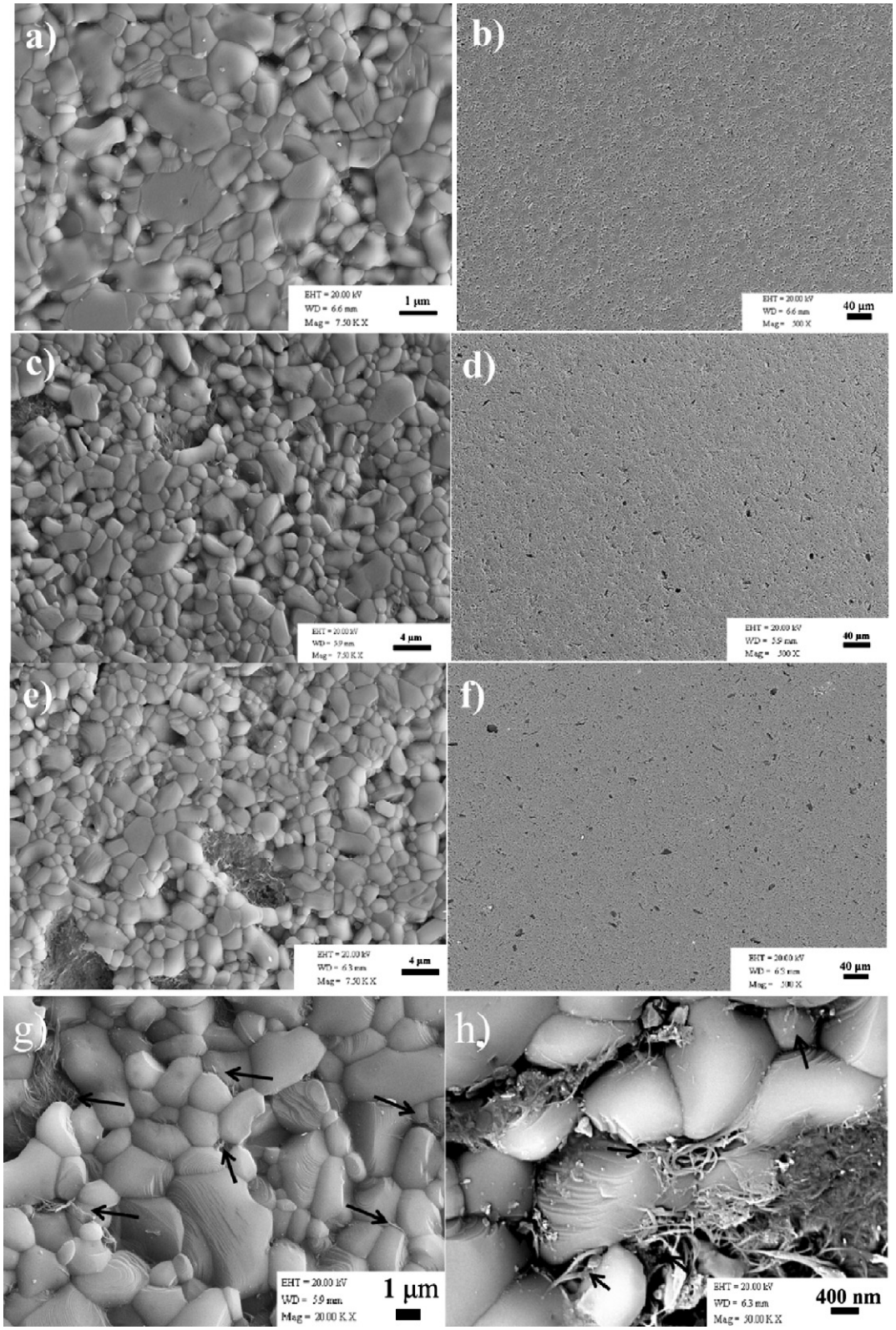

Fig. 2. The polished surfaces of monolithic Al_2O_3 (a) and (b); COOH-SWCNT/Al_2O_3 (c), (d) and (g); OH-SWCNT/Al_2O_3 (e), (f) and (h). The black arrows mark SWCNTs emerging from grain junctions.

electrical conductivities of alumina, COOH-SWCNT/Al_2O_3, and OH-SWCNT/Al_2O_3 are determined to be 2×10^{-6}, 9×10^{-6} and 1.5×10^{-5} S/m, respectively, as shown in Table 2. The electrical conductivity is 4.5 times higher than monolithic alumina for COOH-SWCNT/Al_2O_3 and 7.5 times higher for OH-SWCNT/Al_2O_3.

The limitation of the electrical conductivities lie in moderate levels for SWCNTs reinforced composites, which

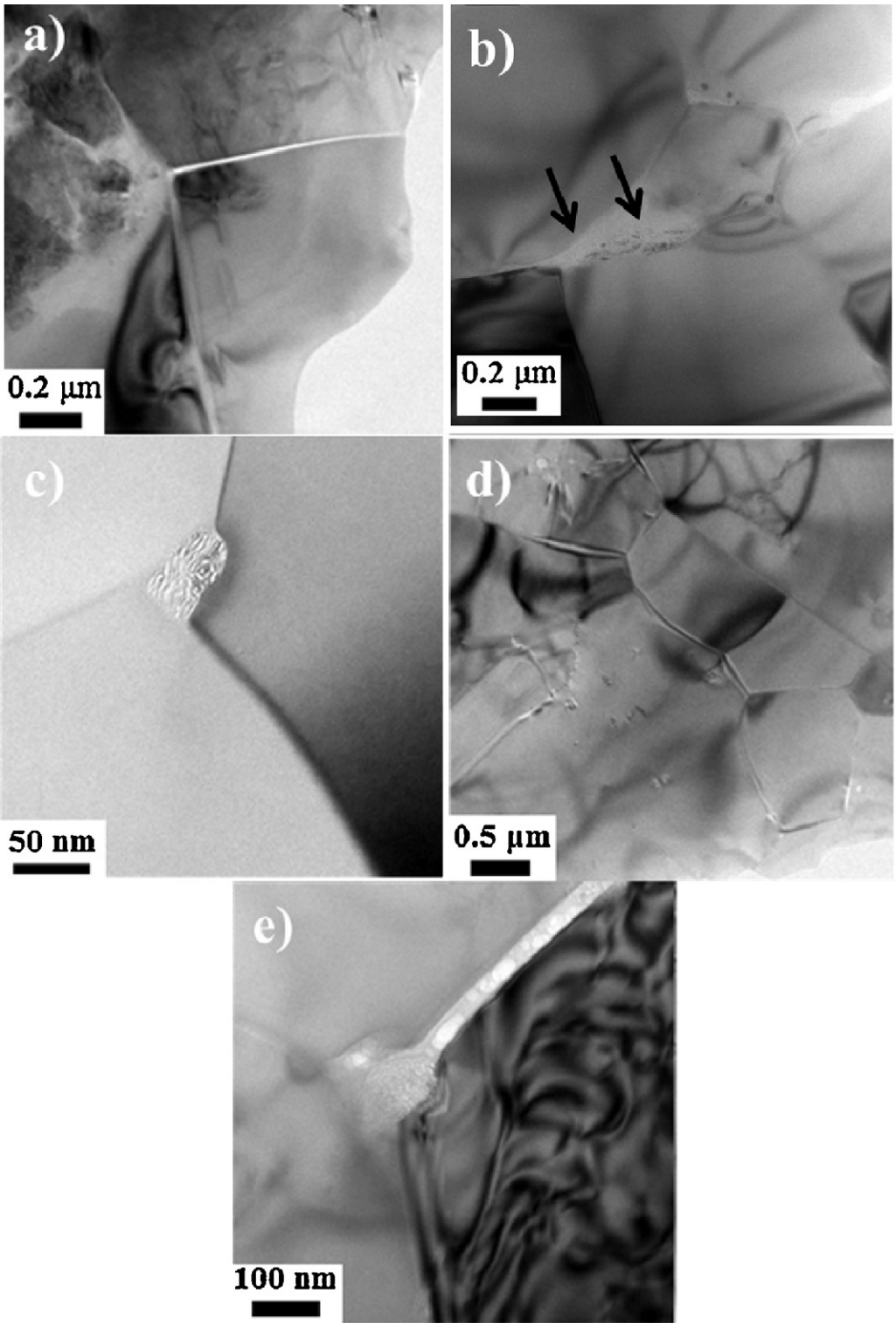

Fig. 3. Transmission electron microscopy (TEM) images of monolithic Al_2O_3 (a), COOH-SWCNT/Al_2O_3 (b–d) and OH-SWCNT/Al_2O_3 (e).

may be attributed to 4 aspects: the low content of SWCNTs, the disruption of their integrity during SPS (since SWCNTs have only single sidewalls, their disruption can be easy), the low crystallinity of carbon nanotubes because of being functionalized and notably the agglomeration of carbon nanotubes.

The toughness increase in the ceramics can be achieved by the addition of nanotubes which results in fibre debonding, fibre pull-out and crack bridging mechanisms which can be confirmed by electron microscopy images. But the agglomeration behaviour of nanotubes unavoidably dictates utilization of toughness measurements and also the electron microscopy

Table 2
The properties of the monolithic alumina and composites.

Material	Processing conditions	Grain size (μm)	Fracture mode	Relative density (%)	Hardness (GPa)	Electrical conductivity (S/m)	Reference
Al_2O_3	SPS (1600 °C 50 MPa 5 min)	3.17	Mixed	99.55	18.7	2×10^{-6}	Present
1 wt.% (1.4 vol%) COOH-SWCNT/Al_2O_3	SPS (1600 °C 50 MPa 5 min)	2.11	Mostly intergranular	97.78	18.5	9×10^{-6}	Present
1 wt.% (1.4 vol%) OH-SWCNT/Al_2O_3	SPS (1600 °C 50 MPa 5 min)	2.28	Mostly intergranular	97.78	18.29	1.5×10^{-5}	Present
Boehmite-derived Al_2O_3	SPS (1600 °C 50 MPa 5 min)	3.25[a]	Mixed	99.9	17.99[b]	10^{-6}[b]	Previous [24]
Boehmite-derived CNT/Al_2O_3 (1 wt.%, 1.87 vol%)	SPS (1600 °C 50 MPa 5 min)	2,42[a]	Mostly intergranular	98	17.28[b]	10^{-2}[b]	Previous [24]
Al_2O_3	SPS (1500 °C 20 MPa 10 min)	1.69		98.6	17.3	10^{-10} to 10^{-12}	[22]
1.9 vol% acid-treated MWCNT/Al_2O_3	SPS (1500 °C 20 MPa 10 min)	1.51		98.9	15.9	1.3	[22]
1.9 vol% pristine MWCNT/Al_2O_3	SPS (1500 °C 20 MPa 10 min)	1.57		98.2	14.4	15.1	[22]
5.7 vol% SWCNT/α-Al_2O_3	SPS (1150 °C/3 min)	~200		100	20.0	1050	[23]

[a] The data obtained but not published yet.
[b] The corrected data of the published paper.

images cannot give numerical values. Now studies are underway to measure the toughness of the samples produced.

Overall, it is shown in the present work that some of the properties of alumina can be changed by the addition of SWCNTs with different surface functional groups. The functional groups increase the solubility of CNTs and hence provide homogeneous dispersion in composites resulting in better properties and refined alumina grains. Further studies are underway to understand the relations between surface functional groups, concentration and the final properties including toughness and wear.

4. Conclusion

Single walled CNTs containing different surface functional groups (COOH and OH) were used for the incorporation into the α-alumina ceramic matrix. SPS was used for the sintering process at 1600 °C for 5 min under 50 MPa pressure. Electron microscopy images show that nanotube addition to alumina shifted the fracture mode towards the intergranular fracture and there is a reduction in grain size from 3.17 μm for monolithic alumina to 2.11 and 2.28 μm for COOH and OH functionalized carbon nanotube containing ceramic bodies, respectively. It is also shown by SEM and TEM observations that carbon nanotubes tend to locate between the grains. The relative density (%) of monolithic alumina is dropped from 99.95 to 97.78 for both composites due to small degree of the agglomeration of CNTs. The electrical conductivity is 4.5 times higher than that monolithic alumina for COOH-SWCNT/Al_2O_3 and 7.5 times higher for OH-SWCNT/Al_2O_3.

The content of different functional groups on CNTs should effect the microstructure and properties of ceramic matrices owing to the difference in the dispersion character of different CNTs, therefore knowing the suitable functional groups to obtain enhanced properties is crucial for obtaining novel ceramic composites. It is shown that COOH or OH functionalized single walled carbon nanotube containing alumina ceramics exhibit similar properties and there is a modest level of increase in electrical conductivities and decrease ingrain size while one is remaining nearly constant (hardness) for both. Therefore it can be concluded that OH or COOH functional group containing nanotubes act or distribute similarly in alumina matrices.

Acknowledgements

This work was funded by TUBITAK (The Scientific and Technological Research Council of Turkey) under the contract number 108T651. Özgür Duygulu from TUBITAK MAM and Mustafa Okutan from Gebze High Technology Institute are also acknowledged for the assistance with TEM studies and electrical conductivity measurements, respectively.

References

[1] P. Boch, J.C. Niepce, Ceramic Materials: Process Properties and Applications, ISTE Ltd., London, 2007.
[2] C.A. Harper, Handbook of Ceramics Glasses and Diamonds, Mcgraw-Hill, New York, 2001.
[3] A. Oberlin, M. Endo, T. Koyama, Filamentous growth of carbon through benzene decomposition, J. Cryst. Growth 32 (1976) 335.
[4] S. Iijima, Helical microtubules of graphitic carbon, Nature 354 (1991) 56–58.
[5] M.M. Treacy, T.W. Ebbesen, J.M. Gibson, Exceptionally high Young's modulus observed for individual carbon nanotubes, Nature 381 (1996) 678–680.
[6] M.F. Yu, O. Lourie, M.J. Dyer, T.F. Kelly, S. Ruoff, Strength and breaking mechanism of multi-walled carbon nanotubes under tensile load, Science 287 (2000), 637-641.
[7] A. Thess, R. Lee, P. Nikolaev, H. Dai, P. Petit, J. Robert, C. Xu, Y.H. Lee, S.G. Kim, A.G. Rinzler, D.T. Colbert, G.E. Scuseria, D. Tomanek, J.E. Fischer, R.E. Smalley, Crystalline ropes of metallic carbon nanotubes, Science 273 (1996) 483–487.
[8] M.J. Biercuk, M.C. Llaguno, M. Radosavlijevic, J.K. Hyun, A.T. Johnson, Carbon nanotube composites for thermal management, Appl. Phys. Lett. 80 (2002) 2767–2769.
[9] J. Cho, A.R. Boccaccini, M.S.P. Shaffer, Ceramic matrix composites containing carbon nanotubes, J. Mater. Sci. 44 (2009) 1934–1951.

[10] M.S.P. Shaffer, X. Fan, A.H. Windle, Dispersion and packing of carbon nanotubes, Carbon 36 (1998) 1603–1612.
[11] E.T. Mickelson, I.W. Chiang, J.L. Zimmerman, P.J.B.J. Lozano, J. Liu, R.E. Smalley, R.H. Hauge, J.L. Margrave, Salvation of fluorinated single-wall carbon nanotubes in alcohol solvents, J. Phys. Chem. B 103 (1999) 4318–4322.
[12] Y.T. Shieh, G.L. Liu, H.H. Wu, C.C. Lee, Effects of polarity and pH on the solubility of acid-treated carbon nanotubes in different media, Carbon 45 (2007) 1880–1890.
[13] F. Inam, H. Yan, M.J. Reece, T. Peijs, Dimethylformamide: an effective dispersant for making ceramic–carbon nanotube composites, Nanotechnology 19 (2008) 195710.
[14] D. Jiang, K. Thomson, J.D. Kuntz, J.W. Agerb, A.K. Mukherjee, Effect of sintering temperature on a single-wall carbon nanotube-toughened alumina-based nanocomposite, Scripta Mater. 56 (2007) 959–962.
[15] J.G. Santanach, A. Weibel, C. Estourne's, Q. Yang, Ch. Laurent, A. Peigney, Spark plasma sintering of alumina: study of parameters, formal sintering analysis and hypotheses on the mechanism(s) involved in densification and grain growth, Acta Mater. 59 (2011) 1400–1408.
[16] M. Meyyappan, Carbon Nanotubes: Science and Applications, CRC Press, New York, 2005.
[17] T. Gómez-del Río, P. Poza, J. Rodríguez, M.C. García-Gutiérrez, J.J. Hernández, T.A. Ezquerra, Influence of single-walled carbon nanotubes on the effective elastic constants of poly(ethylene terephthalate), Compos. Sci. Technol. 70 (2010) 284–290.
[18] N. Ueda, T. Yamakami, T. Yamaguchi, K. Kitajima, Y. Usui, K. Aoki, T. Nakanishi, F. Miyaji, Morinobu Endo, Naoto Saito, S. Taruta, Fabrication and mechanical properties of high-dispersion-treated carbon nanofiber/alumina composites, J. Ceram. Soc. Jpn. 118 (2010) 847–854.
[19] A.C. Zaman, C.B. Ustundag, N. Kuşkonmaz, F. Kaya, C. Kaya, 3-D micro-ceramic components from hydrothermally processed carbon nanotube-boehmite powders by electrophoretic deposition, Ceram. Int. 36 (2010) 1703–1710.
[20] F. Inam, H. Yan, T. Peijs, M.J. Reece, The sintering and grain growth behaviour of ceramic–carbon nanotube nanocomposites, Compos. Sci. Technol. 70 (2010) 947–952.
[21] I. Ahmad, M. Unwin, H. Cao, H. Chen, H. Zhao, A. Kennedy, Y.Q. Zhu, Multi-walled carbon nanotubes reinforced Al_2O_3 nanocomposites: mechanical properties and interfacial investigations, Compos. Sci. Technol. 70 (2010) 1199–1206.
[22] G. Yamamoto, M. Omori, T. Hashida, H. Kimura, A novel structure for carbon nanotube reinforced alumina composites with improved mechanical properties, Nanotechnology 19 (2008) 315708–315715.
[23] G.D. Zhan, A.K. Mukherjee, Carbon nanotube reinforced alumina-based ceramics with novel mechanical, electrical, and thermal properties, Int. J. Appl. Ceram. Technol. 1 (2004) 161–171.
[24] A.C. Zamana, C.B. Üstündag, A. Celik, A. Kara, F. Kaya, Cengiz Kaya, Carbon nanotube/boehmite-derived alumina ceramics obtained by hydrothermal synthesis and spark plasma sintering (SPS), J. Eur. Ceram. Soc. 30 (2010) 3351–3356.